MATHEMATICAL MODELING ON GAS TURBINE BLADES/VANES UNDER VARIABLE CONVECTIVE AND RADIATIVE HEAT FLUX WITH TENTATIVE DIFFERENT LAWS OF COOLING

F. FLORIS[1] & G. VIGLIALORO[2]
[1]Department of Mechanical, Chemical and Material Engineering. University of Cagliari (Italy).
[2]Department of Mathematics and Computer Science. University of Cagliari (Italy).

ABSTRACT

In the last twenty years the modeling of heat transfer on gas turbine cascades has been based on computational fluid dynamic and turbulence modeling at sonic transition. The method is called Conjugate Flow and Heat Transfer (CHT). The quest for higher Turbine Inlet Temperature (TIT) to increase electrical efficiency makes radiative transfer the more and more effective in the leading edge and suction/pressure sides. Calculation of its amount and transfer towards surface are therefore needed. In this paper we decouple convection and radiation load, the first assumed from convective heat transfer data and the second by means of emissivity charts and analytical fits of heteropolar species as CO_2 and H_2O. Then we propose to solve the temperature profile in the blade through a quasi-two-dimensional power balance in the form of a second order partial differential equation which includes radiation and convection. Real cascades are cooled internally trough cool compressed air, so that we include in the power balance the effect of a *heat sink* or *law of cooling* that is up to the designer to test in order to reduce the thermal gradients and material temperature. The problem is numerically solved by means of the Finite Element Method (FEM) and, subsequently, some numerical simulations are also presented.
Keywords: finite element method, gas turbines, heat balance equation, mathematical simulations, radiative/convective heat transfer.

1 INTRODUCTION: MOTIVATIONS, OBJECTIVE AND OUTLINE

In the design of the modern gas turbine (GT) there are still available at least three methods to increase the electric efficiency. These are as follows: (i) Combined cycles applications, (ii) non-conventional ways of blade cooling (mixed steam/air) and (iii) increase in Turbine Inlet Temperature (TIT). On the first two methods please make reference to [1–4]).

The present paper deals with the third item (TIT) through the analysis of the cooling performance of internally air-cooled turbine blades. The TIT can be as high as 1800 K and exceeds the melting temperature of the metal walls. In order to prevent failure and extend the engine endurance, the maximum temperature of the blades/vanes has to be 1300 K or lower. As stated in [5]: "....the peak magnitude of heat transfer coefficient is no longer so important as the gradients in coefficient and material temperature. Higher gradients lead to stress and strain barriers, either steady or cyclic, as well as greater level of thermodynamic unmixedeness or inefficiencies...".

The majority of internal cooling augmentation improvement has dealt with the use of various forms of turbulators and pin fins in internal ducts with the desirable result to increase the heat transfer magnitudes. Anyway these tools come with undesirable increased material thermal gradients (see [6]).

Large temperature gradients have a major effect on mechanical properties. Since Young modulus and coefficient of thermal expansion are temperature dependent, they also vary throughout the body and thermal stress are caused by differential thermal expansion.

ISSN: 2046-0546 (paper format), ISSN: 2046-0554 (online), http://www.witpress.com/journals
DOI: 10.2495/CMEM-V5-N1-55-65

In the last 30 years the gas turbine cooling technology has been based on the simulation of flow around the blade to model the turbulence and predict the laminar-turbulent transition region under transonic conditions.

The above modeling is known as Conjugate Flow and Heat Transfer (CHT) and has been discussed in many papers (see, for instance, [7–9]). The result of the Computational Fluid Dynamics simulation (CFD) offers a convective heat transfer coefficient in the form of a Nusselt number spatial correlation. Radiation is assumed as an increment to it.

In the real GT, radiation flux and convective heat transfer loads are in parallel and only convection is affected by laminar-turbulent transition. Besides, radiation is between 10% and 20% of the heat flux already, and in regions viewing the flame zone is even higher. Since the cooling system has to be designed to withstand the load peak conditions, an alternative method to the CHT could be to assume as boundary condition the maximum radiation load that impact on blade/vanes and the mean convective heat transfer at peak load too.

The objective of the present work is then to evaluate the different cooling pattern performances on the blade temperature and thermal gradients.

We use the method to establish directly the differential form of heat contributions in terms of an appropriately chosen differential control volume by considering the blade as a homogeneous material whose thermal conductivity is independent of temperature, as it was done in [10].

We then introduce in the control volume the rate of energy subtraction as a distributed sink per unit volume and use the terms *heat sink* or *law of cooling* as description of the strength energy subtraction per unit volume; such strength has to be also distributed in the spatial directions. Indeed the way the blades are internally cooled by ducts and ribs properly positioned it has to follow an effective qualitative/quantitative heat subtraction strategy.

In conclusion, we expect that the analysis herein proposed gives information to the designer on how to engineer the cooling inside the blade and, therefore, take advantage on knowing where heat sink is more necessary.

Technically, we model the aforementioned approach throughout the corresponding balance equilibrium in the workpiece, in term of its temperature. Such balance is defined by a quasi-two-dimensional problem, derived in Section 2, which is presented by means of an elliptic partial differential equation in a rectangle, with precise boundary conditions. Through the classical Finite Element Method (FEM) technique the problem is numerically solved and some examples and simulations are analyzed in Section 3. Lastly, the remarks discussed in Section 4 conclude the paper.

2 MODELING THE QUASI-TWO-DIMENSIONAL ENERGY BALANCE WITH RADIATIVE FLUX AND CONVECTION

The radiative heat transmission requires prediction of the radiative properties of transient species (OH, CO, …) and of the main products of combustion, CO_2 and H_2O, whose emissivity values are function of partial pressures, of pressure ratio, of mean free path, of gas and surface metal temperature ([11]). The combustion products emissivity is related to Hottel emissivity with overlapping correction effect.

At the leading edge the heat flux is higher both for the flame proximity (direct radiation heat flux effect) and the stagnation enthalpy. The convective heat flux local values present singularities along the curved variable (in the stagnation point, in transition from laminar to

turbulent, across transonic zones). It appears feasible, in order to write explicitly the heat balance and to solve numerically the temperature field, to preserve partly the variability of heat flux along the curved coordinate. It is done assigning a constant mean value of convective heat transfer along all the blade surface and add at it the radiation flux (variable) given by Hottel charts at boundaries. Radiation is inserted in the boundary conditions and in the first principle statement.

According to Fig. 1, the tip of the blade shroud area is assumed with almost zero heat flux in y direction. Furthermore, the mean blade thickness over the curvilinear coordinate x is less than 0.01 meters and the Biot number based on mean thickness is below 1/6 (see [12]).

Therefore, including into the differential equation the heat transfer load in the third direction z, convection and radiation independently, we obtain the energy balance as a quasi-two-dimensional problem. This means that the variation of the absolute temperature with location in direction z will be slight and can reasonably be approximated as being uniform; hence, setting $\mathrm{x} = (x, y)$, $T = T(\mathbf{x})$, i.e. the temperature is function of x and y, only.

In addition, the total thermal load Q is given by the contribution of radiation Q_R and convection Q_C, i.e.

$$\mathrm{Q} = Q_R + Q_C. \tag{1}$$

Subsequently, as illustrated in Fig. 1, we define the heat flux $Q_R = Q_{R_1} + Q_{R_2}$, where

$$Q_{R_1}/A_L = q_1'' \ (\mathrm{W/m^2}) \text{ and } Q_{R_2}/A_S = q_2'' \ (\mathrm{W/m^2}). \tag{2}$$

Statement 1 *A number of investigations (see, for instance, see [13–15]) offers a tentative way to express analytically the Hottel charts or explores alternative ways. Due to the high non linearity ofgas radiation parameters, it is not possible to provide an explicit relationship for Q_{R_1} and Q_{R_2}, and therefore Q_R. We expect then that radiation Q_R on first stage blades is around 200 W and 400 W. The leading edge is exposed to higher radiation. To these radiation fluxes the convective heat transfer coefficient effect h_∞ has to be added. Even though*

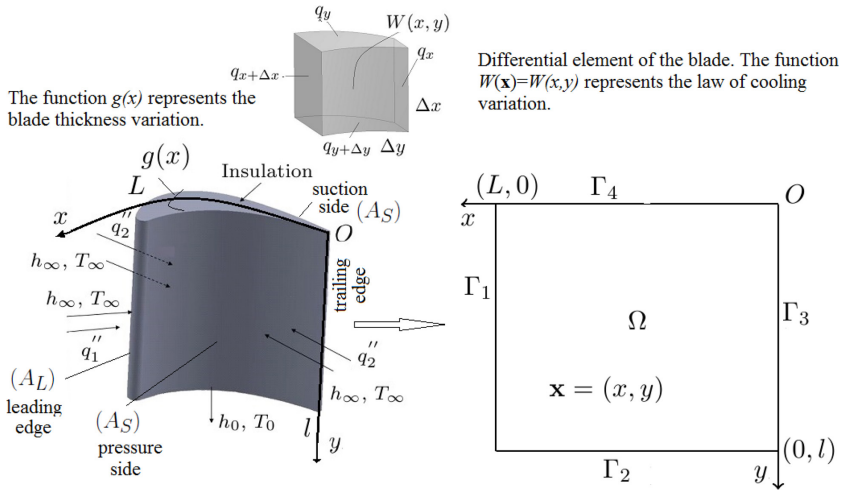

Figure 1: Quasi two-dimensional energy balance. Representation of the turbine blade and definition of the domain of the problem. Γ_1 ($x = L$) stands for the leading edge and Γ_3 ($x = 0$) for the trailing edge of the blade.

the dependence of h_∞ is not easily expressed as an analytical function, we assume for it a reasonable value taken between 150 W/m^{2}K and 400 W/m^{2}K. Therefore, the convection contribution Q_C is from 200 W to 1100 W. These ranges will be considered in the numerical examples presented in Section 3.

2.1 Energy balance problem

In the small element of volume of length Δx and height Δy (Fig. 1), the steady energy balance sums up Fourier fluxes in x and y and convection plus radiation fluxes in the z direction.

By indicating with $W(\mathbf{x})$ the law of cooling that protects the blade from overheating, and taking also into account relation (2) defining flux q_2'', the governing equation for conduction in the blade is written for constant material properties as

$$\begin{aligned}(kg(x)((T(\mathbf{x})-T_\infty)_x)_x\Delta x\Delta y+(kg(x)((T(\mathbf{x})-T_\infty)_y)_y\Delta x\Delta y\\ +2q_2''\,\Delta x\Delta y-2h_\infty(T(\mathbf{x})-T_\infty)\Delta x\Delta y\\ -W(\mathbf{x})g(x)\Delta x\Delta y=0,\ \mathbf{x}\in\Omega,\end{aligned}\tag{3}$$

Ω being the rectangle $[0, L]\times[0, l]$ represented in Fig. 1. Arranging expression (3), we have

$$(x^2T_x)_x+x^2T_{yy}-m^2\,(T-T_\infty)=-n+\tilde{W},\ \mathbf{x}\in\Omega,\tag{4}$$

where these relations

$$m^2=\frac{2h_\infty L^2}{kb},\ n=\frac{2q_2''L^2}{kb},\ \tilde{W}(\mathbf{x})=\frac{x^2W(\mathrm{x})}{k},\ g(x)=b(\frac{x}{L}),\ b(\frac{x}{L})^2,\ b>0,\tag{5}$$

have been considered and where we have defined T_x (respectively T_y) the partial derivative of T with respect to x (respectively y).

Now, in order to totally define the energy balance problem, eqn (4) has to be completed with boundary conditions. Similarly to the internal balance, the sum of Fourier, radiation and convection fluxes at the boundaries of the blade gives (see again Fig. 1):

$$\begin{cases}T_x=\dfrac{q_2''}{k}-\dfrac{h_\infty}{k}\,(T-T_\infty) & \mathbf{x}\in\Gamma_1,\ T==-\dfrac{h_\infty}{k}\,(T-T_0)\ \mathbf{x}\in\Gamma_2,\\ T=T_\infty+q_2''/h_\infty & \mathbf{x}\in\Gamma_3,\ T=0 \qquad\qquad \mathbf{x}\in\Gamma_4.\end{cases}\tag{5}$$

Remark 1 *Being the shroud almost insulated, we applied on Γ_4 the no heat flux boundary condition; in addition, since the idealized model assumes no surface in the line $x = 0$, the temperature on Γ_3 is considered constant as specified in* (5).

2.2 Law of cooling

In this section we infer a tentative heat sink into the blades and vanes in order to reduce heat transfer to metal. Such cooling is sized according to the total thermal impact Q defined in (1) and quantifiable from estimations of Q_R and Q_C in Statement 1. Exactly, we consider this general relation

$$W(\mathbf{x})=\gamma(\mathbf{x})\frac{Q}{V},\tag{6}$$

where $\gamma(\mathbf{x})$ will be later appropriately fixed, V being the volume of the blade.

The skill to solve the boundary problem defined through (4) and (5), moves now the focus of the analysis on material temperature field generated by thermal load Q and how to distribute cooling in order to have smoother material temperatures.

A second step in real GT design would be to engineer the channeling of the convective heat cooling inside the blade according to the law of cooling. We understand the importance to add a film cooling to internal cooling also (see [16–18]). Nonetheless the computational fluid dynamics of the flow field is out of the objective of this work.

3 NUMERICAL EXAMPLES

In this section we carry out some numerical simulations. Hence, according to Statement 1, we then assume for Q_R (more exactly for Q_{R_1} and Q_{R_2}), Q_C and h_∞ assigned values inside the ranges therein specified. In addition, the values assumed as boundaries, gas temperature, surface convection coefficients, cooling fluid temperature, radiation flux, alloy conductivity and geometry of the model blade/vane, are given in Table 1. On the other hand, we use quadratic P_2 -Lagrange splines for the FEM approximation (see [19]) of the temperature T; therefore, the boundary problem given by (3) and (5) is solved according to three different choices of function $\gamma(\mathbf{x})$ appearing in the law of cooling (6).

In particular, as we said, the blade thickness goes according to a quadratic law in the curvilinear x direction; on the contrary, there is no cross section variation along y direction. The dependence of cooling should be then strongly influenced by thickness variation: hence, we assume a larger variation of the law of cooling by x and a weak by y. That is the reason we solve the energy balance with a heat sink function only of x. Of course, our formulation is totally suitable to solve the problem also for more general laws of cooling, depending on both spatial variables.

More precisely, we consider these three expressions:

$$\textit{sin law } \gamma_1(\mathbf{x}) = \sin\left(\frac{4}{5}\pi\frac{x}{L}\right), \textit{ power law } \gamma_2(\mathbf{x}) = \left(\frac{x}{L}\right)^2; \textit{ root law } \gamma_3(\mathbf{x}) = \sqrt{\frac{x}{L}}\,.$$

For each case, first we analyze the temperature distribution on the entire domain Q and then we study the (temperature) profiles and gradients (derivative) for some orthogonal sections on the same domain Q.

Remark 2 *We used the software package FreeFem++ (see [20]). This is a FEM free programming language, that is straightforward to solve problems (both 2D or 3D) from several branches of physics and engineering (see, for instance, [21–23]).*

3.1 Temperature distribution on the entire blade

In Figs 2–4 the color restitutions of the temperature profiles are given in the shape of 2D graphs (left sides) and 3D surfaces (right sides) plots obtained for the three mentioned laws

Table 1: Values of the parameters used in the numerical simulations.

$L = 0.062$ m	$h_0 = 1{,}000$ W/m^2 K	$T_\infty = 1{,}700$ K	$Q_C = 455$ W
$l = 0.066$ m	$k = 12$ W/mK	$T_0 = 400$ K	($Q_R = 210$ W)
$b = 0.014$ m	$q_1'' = 5.10^4$ vW/m^2	$Q_{R_1} = 46$ W	($Q = 665$ W)
$h_\infty = 200$ W/m^{2}K	$q_2'' = 2.10^4$ W/m^2	$Q_{R_2} = 164$ W	

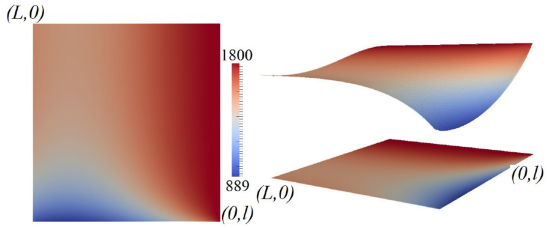

(a) Temperature distribution.

(b) Profile of the law of cooling $W_1(\mathbf{x})$ prescribed in (6).

Figure 2: Numerical results: temperature distribution on the entire blade. Case $\gamma_1(\mathbf{x}) = \sin\left(\frac{4}{5}\pi\frac{x}{L}\right)$.

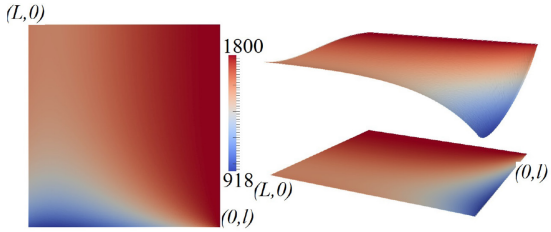

(a) Temperature distribution.

(b) Profile of the law of cooling $W_2(\mathbf{x})$ prescribed in (6).

Figure 3: Numerical results: temperature distribution on the entire blade. Case $\gamma_2(\mathbf{x}) = (x/L)^2$.

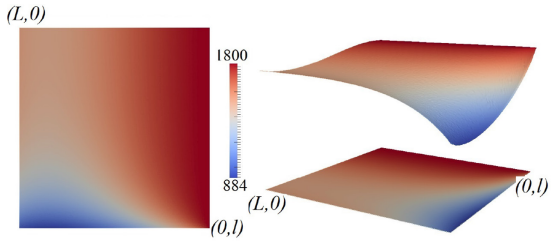

(a) Temperature distribution.

(b) Profile of the law of cooling $W_3(\mathbf{x})$ prescribed in (6).

Figure 4: Numerical results: temperature distribution on the entire blade. Case $\gamma_3(\mathbf{x}) = \sqrt{x/L}$.

of cooling. The high temperature wave moves from the trailing edge inwards vertically and axially in all cases as it is not affected by any cooling. This phenomenon is expected due the singularity of the border. In real turbomachinery the trailing edge has to be film cooled. The different formulations of heat sink shapes have no effect on this border, as they are equal zero at $x = 0$. Staying close to the leading edge and moving inwards, apparently the progressive effect of the sin law is more effective than it is the power law. The root law plays itself in between. The penetration of the heat wave from the stagnation point is efficiently blocked

by the subtraction of heat given both by the cool wave from below and from the heat sink according to functions $\gamma_1(\mathbf{x})$, $\gamma_2(\mathbf{x})$ and $\gamma_3(\mathbf{x})$.

3.2 Temperature profiles and gradients

In Fig. 5 the values of temperature T (y) are shown in four sections taken in $x = L/3$, $x = L/2$, $x = 2L/3$ and $x = L$. The higher values of temperature are shown close to the trailing edge. Analogously, at $y = 0$ position, the temperature is higher and decreases as the cooling effect from below moves up. The temperature could easily kept lower with an higher amount of heat sink. The main difference in the results is still found near the trailing edge border and insulation surface. In all cases temperature changes appreciably near the cooled root. For all the T (y) obtained, the $\sin\left(\frac{4}{5}\pi\frac{x}{L}\right)$ performs better, followed by the $\sqrt{x/L}$ law and then the $(x/L)^2$ gives apparently the poorest result. Figure 6 shows the absolute gradients (derivative) of T with respect to y, at flat planes taken at four different x values: $L/3$, $L/2$, $2L/3$ and L. The thermal wave induced by the cooled border at $y = l$ does not reach the alloy matrix deep into the core, as gradients are very high close to the platform. The cool wave is able to keep metal cooled only close to the root and then, moving up towards the height center and beyond towards the adiabatic shroud, gradients become lower and temperature decisively higher. Gradients are not affected by the different law of cooling. There are two possible

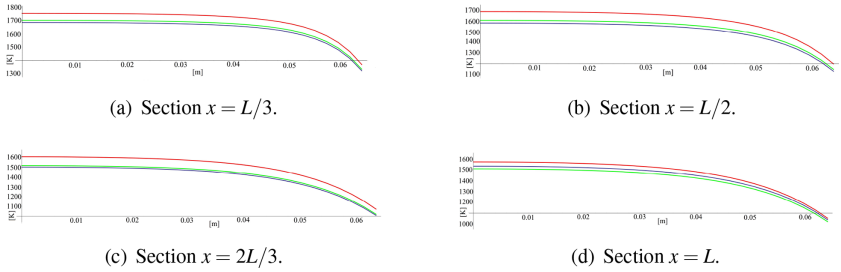

(a) Section $x = L/3$. (b) Section $x = L/2$.

(c) Section $x = 2L/3$. (d) Section $x = L$.

Figure 5: Numerical results: temperature profiles for fixed sections along x direction. The blue line represents the result attained in the case of the *sin law* (i.e. γ_1 **(x)),** the red of the *power law* (i.e. γ_2 **(x))** and the green of the *root law* (i.e. γ_3**(x))**.

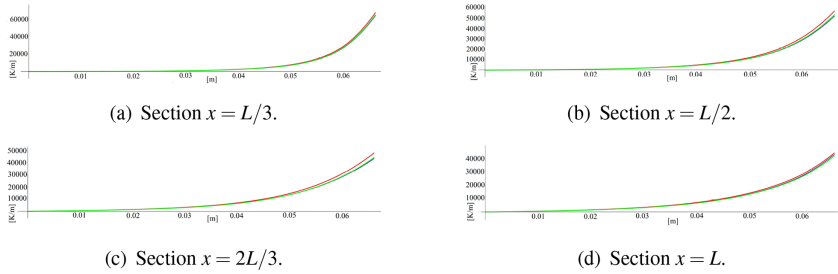

(a) Section $x = L/3$. (b) Section $x = L/2$.

(c) Section $x = 2L/3$. (d) Section $x = L$.

Figure 6: Numerical results: temperature gradients for fixed sections along x direction. The blue line represents the result attained in the case of the *sin law* (i.e. $\gamma_1(\mathbf{x})$**),** the red of the *power law* (i.e. $\gamma_2(\mathbf{x})$) and the green of the *root law* (i.e. $\gamma_3(\mathbf{x})$).

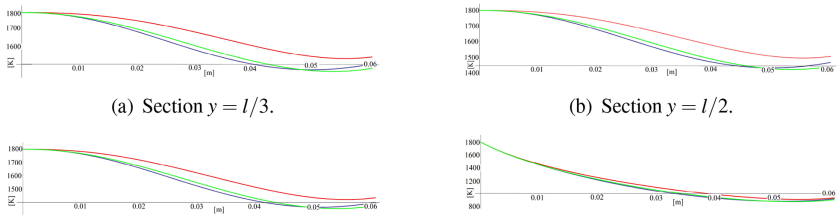

(a) Section $y = l/3$. (b) Section $y = l/2$.

(c) Section $y = 2l/3$. (d) Section $y = l$.

Figure 7: Numerical results: temperature profiles for fixed sections along y direction. The blue line represents the result attained in the case of the *sin law* (i.e. γ_1 (**x**)), the red of the *power law* (i.e. γ_2(**x**)) and the green of the *root law* (i.e. γ_3(**x**)).

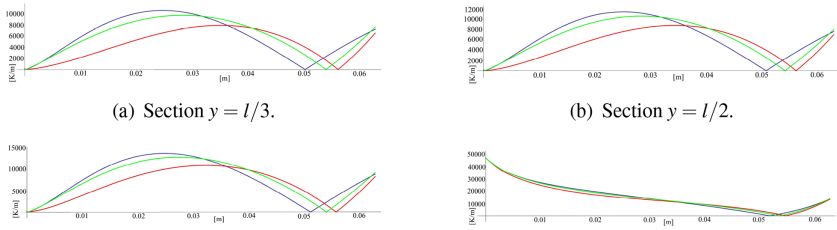

(a) Section $y = l/3$. (b) Section $y = l/2$.

(c) Section $y = 2l/3$. (d) Section $y = l$.

Figure 8: Numerical results: temperature gradients for fixed sections along y direction. The blue line represents the result attained in the case of the sin *law* (i.e. γ_1(**x**)), the red of the *power law* (i.e. γ_2(**x**)) and the green of the *root law* (i.e. γ_3(**x**)).

explanations to this effect: the low alloy thermal conductivity and the unbalance between the amount of heat sink in the core and the thermal load induced by the cooled platform.

Similarly, in Fig. 7 the values of temperature *T (x)* are shown for four sections taken in $y = l/3$, $y = l/2$, $y = 2l/3$ and $y = l$. The boundary at the point $x = 0$, where the blade idealization has no area, forces the metal temperature to be higher than the gas temperature value, i.e. equal to $T_\infty + q_2''/h_\infty$ (see the third condition in (5)). It would mean to implement the total cooling flow rate and to distribute it according to the law of cooling. The *T (x)* results versus one-thirds chord plane, midplane chord, two-thirds chord plane and root plane edge rise up a bit as *x* reaches the leading edge. For all the *T(x)* values the $\sin\left(\frac{4}{5}\pi\frac{x}{L}\right)$ performs better but at the extreme stagnation point. The plot reverses at about *x/L* = 5/8, where the sin law starts to decrease as the consequence of the form given to the sin law maximum at five eights of *L*.

Another observation has to be made from Fig. 8: close to the cooled lower bound, the temperature gradients are decisively low and weakly dependent by cooling low. A different plot is given deep into the blade core: the gradients rise up and the performances of the heat sink effect are now reversed. The $\sin\left(\frac{4}{5}\pi\frac{x}{L}\right)$ law has the lower performances. At $y = l$ the behavior is almost unchanged for all the three laws of cooling. As *y* moves away from the cooling root lower boundary, the gradient of temperature dramatically increases at midplane. The best gradient performance is assigned to the sin(4 nL) heat sink when $x \geq L/2$. As the solution reaches the leading edge bound, it is possible that temperature solution is affected by the substantial increment in the heat load due to the flux q_1'' previously defined.

4 CONCLUDING REMARKS

The present work considers the first principle, steady, of energy balance in a blade/vane gas turbine alloy affected by parallel convection and radiation heat fluxes.

The quasi-two-dimensional approach is implemented as Biot number based on mean thickness is lower than 1/6. The energy balance is modeled by means of an elliptic problem, with mixed boundary conditions. This approach tends to simplify the conjugate and heat transfer analysis of transient flow with unknown heat flow, heat transfer coefficient and uncertainty in radiative amount contribution. It is concluded that the FEM strategy is much easier to implement as compared to the full conjugate problem to solve. In fact, once the partial differential problem is solved the solution is valuable because it provides a mean to infer the temperature field when a distribution of cooling effect is assigned to the domain. Specifically, through the paper, three hypothesis of law of cooling are successfully investigated. The solutions are easily available to the insertion of general laws of cooling of different type. The discussed results, indeed, show that the chosen laws of heat subtraction have to be better balanced. In the meantime the heat sink in the form of power, root and sin law are good analytical expressions to use as starting base for improvements.

ACKNOWLEDGMENTS

Viglialoro is member of the Gruppo Nazionale per l'Analisi Matematica, la Proba-bilita e le loro Applicazioni (GNAMPA) of the Istituto Nazionale di Alta Matematica (INdAM) and gratefully acknowledges the Italian Ministry of Education, University and Research (MIUR) for the financial support of Scientific Project "Smart Cities and Communities and Social Innovation – ILEARNTV anywhere, anytime – SCN_bb3b7".

NOMENCLATURE

A_L	Area of the leading edge	[m^2]
A_S	Area of the suction/pressure side	[m^2]
h_0	Cooling fluid convective heat transfer coefficient	[W/m^{2}K]
h_∞	Convective heat transfer coefficient	[W/m^{2}K]
k	Thermal conductivity	[W/mK]
$Q_{,,}$	Total thermal load	[W]
q_1''	Heat flux on the leading edge	[W/m^2]
q_2	Heat flux on the suction/pressure side	[W/m^2]
Q_C	Convective thermal load	[W]
Q_R	Total radiation thermal load	[W]
Q_{R1}	Radiation thermal load acting on AL	[W]
Q_{R2}	Radiation thermal load acting on AS	[W]
T	Absolute gas temperature	[K]
T_0	Cooling fluid temperature	[K]
T_∞	Turbine inlet temperature	[K]
V	Volume of the blade	[m^3]

REFERENCES

[1] Chiesa, P., Lozza, G., Macchi, E. & Consonni, S., An assessment of the thermodynamic performance of mixed gas-steam cycles: part b: water-injected and HAT cycles. *Journal of Engineering for Gas Turbines and Power,* **117**(3), pp. 499–508, 1995. http://dx.doi.org/10.1115/1.2814123

[2] Eckardt, D. & Rufli, P., Advanced gas turbine technology - ABB/BBC historical firsts. *Journal of Engineering Gas Turbines and Power,* **124**(3), pp. 542–549, 2002. http://dx.doi.org/10.1115/1.1470484
[3] Gaul, G.R., Diakunchak, I.S. & Dodd, A.M., The W5b1G testing and validation in the Siemens Westinghouse advanced turbine systems program. *ASME Proceedings Electric Power,* Paper 2001-GT-0399, 2011.
[4] Macchi, E., Consonni, S., Lozza, G. & Chiesa, P., An assessment of the thermodynamic performance of mixed gas-steam cycles: part a-intercooled and steam-injected cycles. *Journal of Engineering for Gas Turbines and Power,* **117**(3), pp. 489–498, 1995.
[5] Bunker, R.S., Gas turbine heat transfer: ten remaining hot gas path challenges. *Journal of Turbomachinery,* **129**(2), pp. 193–201, 2006. http://dx.doi.org/10.1115/1.2464142
[6] Han, J.C. & Wright, L.M., *Enhanced Internal Cooling of Turbine Blades and Vanes.* The Gas Turbine Handbook, U.S., National Energy technology Laboratory, Morgantown. Section 4.2.2.2. 2007.
[7] Alhajeri, M. & Alhamad Alhajeri, H., Heat and fluid flow analysis in gas turbine cooling passages with semicircular turbulators. *International Journal of Physical Science.* **4**(12), pp. 835–845, 2009.
[8] Akhter, M.N. & Funakazi, K., Development of prediction method of boundary layer bypass transition using intermittency transport equation. *International Journal of Gas Turbine, Propulsion and Power Systems (JGPP),* **1**(1), pp. 30–37, 2007.
[9] Bhaskaran, R. & Lele, S.K., Heat transfer prediction in high pressure turbine cascade with free-stream turbulence using LES. *41st AIAA Fluid Dynamics Conference and Exhibit,* 27–30 June 2011, Honolulu, Hawaii. http://dx.doi.org/10.2514/6.2011-3266
[10] Floris, F., Ilemin, B. & Orrii, P.F., Quasi 1-D analysis of heat equation with exact solutions and comparison with numerical simulation in liquid/vapour pressure tanks, waterwalls and hot drawing machines. *31st UITHeat Transfer Conference,* 25–27 June 2013, Como, Italy.
[11] McAdams, W.H., *Heat Transmission,* 3 edn., McGraw-Hill, 1954.
[12] Rohsenow, W.R. & Choi, H., *Heat, Mass, and Momentum Transfer,* Prentice-Hall, Inc, 1961.
[13] Bueters, K.A., Cogoli, J.C. & Habelt, W.W., Performance prediction of tangentially fired utility furnaces by computer model. *Symposium International on Combustion,* **15,** pp. 1245–1260, 1975. http://dx.doi.org/10.1016/s0082-0784(75)80387-0
[14] Incropera, F.P. & De Witt, D.P., *Fundamentals of Heat and Mass Transfer,* 5 edn, John Wiley & Sons: New York, 2001.
[15] Mehrotra, A.K., Karan, K. & Behie, L.A., Estimate gas emissivities for equipment and process design. *Chemical Engineering Progress,* **91**, pp. 70–77, 1995.
[16] Gao, Z., Narzary, D.P. & Han, J.C., Film-cooling on a gas turbine blade pressure side or suction side with compound angle shaped holes. *Journal of Turbomachinery,* **131**(1), p. 11, 2008.
[17] McElroy, M.W., Lawrie, A. & Bond, I.P., Optimisation of an air film cooled CFRP panel with an embedded vascular network. *International Journal of Heat Mass Transfer.* **88,** pp. 284–296, 2015. http://dx.doi.org/10.1016/j.ijheatmasstransfer.2015.04.071

[18] Wright, L.M., McClain, S.T. & Clemenson, M.D., Effect of density ratio on flat plate film cooling with shaped holes using PSP. *Journal of Turbomachinery,* **133**(4), p. 11, 2011.

[19] Zienkiewicz, O.C. & Taylor, R.L., *The Finite Element Method,* Butterworth-Heinemann, 2000.

[20] Hecht, F., Pironneau, O., Le Hyaric, A. & Ohtsuda, K., *FreeFem++ (Third Edition, Version 3.19).* Laboratoire Jacques-Louis Lions, Universite Pierre et Marie Curie, Paris, available at: http://www.freefem. org/ff++/

[21] Díaz Moreno, J.M., García Vazquez, C., Gonzalez Montesinos, M.T., Ortegon Gallego, F. & Viglialoro, G., Mathematical modeling of heat treatment for a steering rack including mechanical effects. *Journal Numerical Mathematics,* **20**(3–4), pp. 215–232, 2012.

[22] Viglialoro, G., Gonzalez, A. & Murcia, J., A mixed finite-element finite-difference method to solve the equilibrium equations of a prestressed membrane. *International Journal of Computer Mathematics*, available at: http://www.tandfonline.com/doi/pdf/10.1080/00207160.2016.1154950, 2016.

[23] Viglialoro, G. & Murcia, J., Á singular elliptic problem related to the membrane equilibrium equations. *International Journal of Computer Mathematics,* **90**(10), pp. 2185–2196, 2013.
http://dx.doi.org/10.1080/00207160.2013.793317